



## *Acanthopanax senticosus* Harms improves Parkinson's disease by regulating gut microbial structure and metabolic disorders

Yi Lu <sup>a,1</sup>, Xin Gao <sup>b,1</sup>, Yang Nan <sup>b</sup>, Shadi A.D. Mohammed <sup>a,c</sup>, Jiaqi Fu <sup>a</sup>, Tianyu Wang <sup>a</sup>, Chongzhi Wang <sup>d</sup>, Chunsu Yuan <sup>d</sup>, Fang Lu <sup>a,\*\*</sup>, Shumin Liu <sup>a,\*</sup>

<sup>a</sup> Institute of Traditional Chinese Medicine, Heilongjiang University of Chinese Medicine, Harbin, Heilongjiang, China

<sup>b</sup> School of Pharmacy, Heilongjiang University of Chinese Medicine, Harbin, Heilongjiang, China

<sup>c</sup> School of Pharmacy, Lebanese International University, 18644, Sana'a, Yemen

<sup>d</sup> Tang Center for Herbal Medicine Research, and Department of Anesthesia and Critical Care, University of Chicago, Chicago, USA

### ARTICLE INFO

#### Keywords:

*Acanthopanax senticosus* Harms  
Parkinson's disease  
Metabolomics  
Metagenomics  
Gut microbes

### ABSTRACT

Parkinson's disease (PD) is the second most common neurodegenerative disease, with an increasing prevalence as the population ages, posing a serious threat to human health, but the pathogenesis remains uncertain. *Acanthopanax senticosus* (Rupr. et Maxim.) Harms (ASH) (aqueous ethanol extract), a Chinese herbal medicine, provides obvious and noticeable therapeutic effects on PD. To further investigate the ASH's mechanism of action in treating PD, the structural and functional gut microbiota, as well as intestinal metabolite before and after ASH intervention in the PD mice model, were examined utilizing metagenomics and fecal metabolomics analysis.  $\alpha$ -syn transgenic mice were randomly divided into a model and ASH groups, with C57BL/6 mice as a control. The ASH group was gavaged with ASH (45.5 mg/kg/d for 20d). The time of pole climbing and autonomous activity were used to assess motor ability. The gut microbiota's structure, composition, and function were evaluated using Illumina sequencing. Fecal metabolites were identified using UHPLC-MS/MS to construct intestinal metabolites. The findings of this experiment demonstrate that ASH may reduce the climbing time of PD model mice while increasing the number of autonomous movements. The results of metagenomics analysis revealed that ASH could up-regulated *Firmicutes* and down-regulated *Actinobacteria* at the phylum level, while *Clostridium* was up-regulated and *Akkermansia* was down-regulated at the genus level; it could also recall 49 species from the phylum *Firmicutes*, *Actinobacteria*, and *Tenericutes*. Simultaneously, metabolomics analysis revealed that alpha-Linolenic acid metabolism might be a key metabolic pathway for ASH to impact in PD. Furthermore, metagenomics function analysis and metabolic pathway enrichment analysis revealed that ASH might influence unsaturated fatty acid synthesis and purine metabolism pathways. These metabolic pathways are connected to ALA, Palmitic acid, Adenine, and 16 species of *Firmicutes*, *Actinobacteria*, and *Tenericutes*. Finally, these results indicate that ASH may alleviate the movement disorder of the PD model, which may be connected to the regulation of gut microbiota structure and function as well as the modulation of metabolic disorders by ASH.

\* Corresponding author.

\*\* Corresponding author.

E-mail addresses: [lufang\\_1004@163.com](mailto:lufang_1004@163.com) (F. Lu), [keji-liu@163.com](mailto:keji-liu@163.com) (S. Liu).

<sup>1</sup> These authors contributed equally to this work and share first authorship.

## 1. Introduction

Parkinson's disease (PD) is a prevalent neurodegenerative disease characterized by progressive degeneration of dopaminergic neurons in the substantia nigra due to  $\alpha$ -synuclein misfolding, resulting in impaired striatal dopamine release and decreased dopamine levels [1]. Patients with PD often have movement disorders such as resting tremors, myotonia, abnormal walking, and delayed mobility [2]. As the disease advances, patients have significant gastrointestinal dysfunction, cognitive impairment, and psychiatric disorders, all of which reduce their quality of life [3]. It has been found that metabolic disorders caused by an imbalance of gut microbiota may have a role in the development of PD [4].

The enteric nervous system is one of the first and most frequently affected structures by  $\alpha$ -synuclein in PD, and microorganisms located at the intersection of the intestinal lumen and enteric nervous system induce misfolding of  $\alpha$ -synuclein and propagate to neurons in the brain via the vagus nerve [5]. There is a direct correlation between the abundance of *Coriobacteriaceae*, *Corynebacteriaceae*, and *Enterobacteriaceae* in the gut of PD patients and the severity of mobility difficulties, gait rigidity, and postural instability [6,7]. Furthermore, gut microbes may interact with the autonomic and central nervous systems through metabolic and other pathways to alter the PD process [6]. Numerous metabolomic studies have confirmed that the metabolites and metabolic pathways changed dramatically when the gut microbial structure was altered. Lipopolysaccharides, for example, cross the blood-brain barrier into the brain through diffusion and cytokine transport proteins when gut homeostasis and permeability change, breaking the blood-brain barrier's integrity and triggering neuroinflammation [8,9]. In addition, short-chain fatty acids produced by gut microbes may affect neurotransmitter production and receptor expressions, such as dopamine or gamma-aminobutyric acid, influencing the progression of PD. In PD patients, glycolysis is substantially inhibited, and not only is energy metabolism impaired, and the body's ATP level is significantly lowered [10]. Therefore, maintaining the stability of intestinal flora and metabolism is an important factor in ensuring individuals' health, and targeting the intestinal flora and metabolic pathways may be a potential therapeutic for treating and preventing PD.

The medicinal parts of the Chinese herbal medicine *Acanthopanax senticosus* (Rupr. et Maxim.) Harms are dried roots and rhizomes or stems, which are beneficial for replenishing qi to invigorate the spleen, and tonifying the kidney to relieve mental strain. Many studies have shown that ASH mainly consists of terpenoids compounds like eleutheroside B; lignans compounds such as eleutheroside E, sesamin and eugenin; flavonoids such as hypericin, quercetin and rutin; coumarin compounds such as isozainpyridine; and immunostimulating complex polysaccharides and glycans (eleutherosans A-G) [56,57]. Eleutheroside B and eleutheroside E are the main active components of ASH [58,59]. Eleutheroside B has a protective effect on MPP<sup>+</sup>-induced PC12 cell damage [60]. Eleutheroside E activates PKA/CEB/BDNF signal transduction to protect hippocampal neurons [58], and it is associated with monoamine oxidase B with high intensity, and can effectively carry out monoamine oxidase B, which is a very potential drug candidate for PD [61]. Eleutheroside B and eleutheroside E also have immune regulation [62], anti-inflammatory, antioxidant stress and neuroprotective effects [59,63–65]. According to the Chinese Pharmacopoeia 2020 edition, eleutheroside B is the index component of ASH, and its concentration must be more than 0.050% [66]. Previous research found that ASH may regulate peripheral system metabolism to play an anti-oxidative stress role [11] and down-regulate the expression of  $\alpha$ -synaptic [12], as well as preserve the structure and function of mitochondria [13] that play an anti-Parkinsonian role. In this study, we used the PD model  $\alpha$ -syn transgenic mice, the Illumina platform, and UPLC-MS/MS to perform metagenomics sequencing and metabolomics analysis on intestinal contents to further clarify the effect and potential mechanism of ASH in the treatment of PD, as well as to provide new ideas and methods for preventing and treating PD.

## 2. Material

### 2.1. ASH's preparation and UPLC-MS analysis

*Acanthopanax senticosus* (Lot No. 170634) was obtained from Wuchang County, Heilongjiang, and was identified using Chinese Pharmacopoeia (2020). ASH was extracted with 10 times the quantity of 80% ethanol at reflux three times for 2 h each, condensed by rotary evaporation to 500 g/L (in raw drug quantity), and separated and purified using AB-8 macroporous adsorbent resin. The adsorption flow rate was 2 BV/h, and it was eluted with 30% ethanol at 9 BV at a flow rate of 1 BV/h before being concentrated by rotary evaporation and dried [14]. The medicine was then preserved at Heilongjiang University of Chinese Medication's Institute of Chinese Medicine's Research Laboratory of the Theory of Chinese Medicinal Properties (20190702). During the experiment, the dried powder stated above was dissolved in a 0.5% CMC-Na solution. The ASH extract was analyzed using Acquity TH UPLC and High Definition MS system. A suitable amount of ASH extract was weighed and diluted with methanol to 1 mg/ml for injection. Chromatographic conditions: AQUITY UPLC® HSS T3 column (100 mm × 2.1 mm, 1.8  $\mu$ m); Mobile phase A: 0.1% formic acid - aqueous solution, mobile phase B: acetonitrile. Gradient elution: 0–12 min, 100%–60%A, flow rate: 0.5 ml/min. Detection wavelength: 210–500 nm, sample size: 1  $\mu$ l. Mass spectrum conditions: electrospray ion source (ESI), using positive ion mode detection, capillary voltage: 2000 V, sample cone hole voltage: 30 V, ion source temperature: 120 °C, desolvation Temp: 500 °C. The scanning mode is full scanning, and the mass scanning range is mass/charge ratio ( $m/z$ ) 50–1500.

### 2.2. Animals

Nine male C57BL/6 mice and eighteen  $\alpha$ -Syn transgenic male C57BL/6 mice (8 weeks, SPF, body weight  $20 \pm 2$  g), purchased from

Jiangsu JicuiYaokang Laboratory Animal Technology Co., Ltd., license number: SCXK (Su) 2018-0008. The mice were raised at Heilongjiang University of Traditional Chinese Medicine's Experimental Animal Center. The rearing environment's temperature was kept at  $22 \pm 1$  °C, the relative humidity was maintained at  $50\% \pm 5\%$ , and the light/dark cycle was cycled for 12 h/12 h. The mice were given a standard chow and water ad libitum throughout the experiment. The Laboratory Animal Ethics Committee of Heilongjiang University of Traditional Chinese Medicine authorized this experiment in accordance with the Law on the Protection of Laboratory Animals (Directive 86/609/EEC).

After 7d of adaptive feeding,  $\alpha$ -syn transgenic mice were randomly divided into a model group (PD group), ASH group (ASH group), and C57BL/6 mice served as a control group (Con group), with 9 mice in each group. The ASH group was gavaged with ASH extract (45.5 mg/kg/d), while the Con and PD groups were given the same amount of 0.5% CMC-Na solution. In this experiment, the yield of powder was 1.296%, and the body surface area ratio between mice and humans was 9.1, so the dose of ASH was the optimal dose of 45.5 mg/kg (equivalent to 3.5 g/kg crude drug), which was the best effective dose investigated in our previous study [11,14], and it was administered to the mice continuously for 20d.

### 2.3. Sample collection and preparation

All procedures were conducted under aseptic conditions. 24 h after the last administration, mice were anesthetized by injection of 1% sodium pentobarbital and subsequently executed. The contents of the end of the cecum of 3 mice in each group were taken and placed in sterile centrifuge tubes, snap frozen in liquid nitrogen, and stored at  $-80$  °C for intestinal flora MacroGen sequencing. The cecum contents of the remaining 6 mice were added to a pre-cooled methanol/acetonitrile/water solution (2:2:1, v/v), vortexed and mixed, sonicated at low temperature for 30 min, left to stand at  $-20$  °C for 10 min, centrifuged at 14,000 g for 20 min at 4 °C, the supernatant was vacuum dried, then 100  $\mu$ L of acetonitrile aqueous solution (acetonitrile: water = 1:1, v/v) was added, vortexed and centrifuged at 14,000 g for 15 min at 4 °C. The supernatant was used for UPLC-MS/MS analysis.

## 3. Methods

### 3.1. Behavioral observations

#### 3.1.1. Pole climbing experiment

The Pole climbing test is used to assess mice's coordination abilities. A wooden pole with a length of 50 cm and a diameter of 1.5 cm was selected and taped around it to prevent mice from sliding as they climbed the pole. Throughout the adaptive feeding, the mice were led to climb from the top to the bottom of the pole, and they were trained once a week during the administration period. The mice were held by the tail so that all of their limbs were at the top of the pole and their heads were facing downwards, and then allowed to climb down freely. A timer was used to time the mice as they climbed the pole [14,15]. The timer started when the mice stood at the top of the pole and ended when their two forelimbs contacted the platform at the bottom. Each mice climbed three times, at least 30 min apart. If the mice slipped or jumped off the pole, the time was not recorded and had to be remeasured at least 30 min later.

#### 3.1.2. Autonomous activity experiment

The mice were placed in an autonomous activity counter (Beijing Jinotai Technology Development Co., LTD., Model: ZZ-6), one in each cell, and permitted to move freely. Cover the lid and let the mice to adjust to the dark and quiet environment for 2 min before running, and the instrument automatically record the mice's free activity status within 5 min [15]. The machine recorded one additional vertical movement each time the mice stood upright and one more horizontal direction for each walking step. The overall autonomous activity is indicated by vertical and horizontal movement; hence the number of independent activities is the sum of the vertical and horizontal direction. Following the end of each group, the instrument was promptly washed with an alcohol towel to prevent the odor of the previous group of mice from interfering with the movement of the next group of mice, and the next series of studies began after the alcohol had evaporated.

### 3.2. Metagenome sequencing analysis

In this study, based on the Illumina NovaSeq high-throughput sequencing platform, we extracted total genomic DNA from the intestinal flora macro-genome using a Whole Genome Shotgun strategy and constructed libraries of inserts of suitable lengths, which were paired-end sequenced. FastQC was used to screen the raw data for removing unwanted sequences to obtain a high-quality dataset that could be used for downstream macrogenomic analysis. Species annotation of non-spliced sequences was performed using Kaiju. The sequence splicing was performed using MEGAHIT, and sequences were merged, spliced, and de-redundant using the software minimap2 and MMseqs2. The contigs sequences were compared with the NCBI nt database (v2019.8.12) by BLASTN using the "Lowest Common Ancestor (LCA)" algorithm in Blast2lca software to obtain the contigs sequences and annotate the spliced sequences with species information tables. MetaGeneMark software (<http://exon.gatech.edu/GeneMark/>) and protein sequence clustering were used for gene prediction. Subsequently, the protein sequences were functionally annotated with the Kyoto Encyclopedia of Genes and Genomes (KEGG, <https://www.genome.jp/kegg/>) database to obtain functional taxon abundance profiles for each class.

### 3.3. Metabolomics analysis

The samples were separated by an Agilent 1290 Infinity LC ultra-high performance liquid chromatography (UHPLC) system and HILIC column; the column temperature was 25 °C; the flow rate was 0.5 mL/min; the injection volume was 2  $\mu$ L; the mobile phase composition A: water + 25 mM ammonium acetate + 25 mM ammonia, B: acetonitrile; gradient elution program as follows: 0–0.5 min, 95% B; 0.5–7 min, B linearly changing from 95% to 65%; 7–8 min, B linearly changing from 65% to 40%; 8–9 min, B maintained at 40%; 9–9.1 min, B linearly changed from 40% to 95%; 9.1–12 min, B maintained at 95%; the sample was automatically injected at 4 °C during the entire analysis process in the device. To avoid the influence caused by the fluctuation of the instrument detection signal, the continuous analysis of the samples is carried out in random order. QC samples are inserted into the sample queue to monitor and evaluate the system's stability and experimental data's reliability.

An AB Triple TOF 6600 mass spectrometer was used to collect the primary and secondary spectra of the samples. The ESI source conditions after HILIC chromatographic separation were as follows: Ion Source Gas1 (Gas1): 60, Ion Source Gas2 (Gas2): 60, Curtain gas (CUR): 30, source temperature: 600 °C, IonSapary Voltage Floating (ISVF)  $\pm$ 5500 V (both positive and negative modes); TOF MS scan  $m/z$  range: 60–1000 Da, product ion scan  $m/z$  range: 25–1000 Da, TOF MS scan accumulation time 0.20 s/spectra, and product ion scan accumulation time is 0.05 s/spectra; secondary mass spectra were obtained using information-dependent acquisition (IDA) and in high sensitivity mode, Declustering potential (DP):  $\pm$ 60 V (both positive and negative modes), Collision Energy: 35  $\pm$  15 eV, IDA settings, as follows, Exclude isotopes within 4 Da, Candidate ions to monitor per cycle: 10. monitor per cycle: 10.

The raw data in Wiff format were converted to mzXML format by ProteoWizard, and then XCMS software was used for peak alignment, retention time correction, and extraction of peak areas. Unsupervised statistical analysis was performed using principal components analysis (PCA). Then, Orthogonal Partial Least Squares-Discriminant Analysis (OPLS-DA) was used to characterize the metabolic disturbances caused by compound adversative. Variable Importance Projection (VIP) > 1 and  $P < 0.05$  were screening criteria to find potential characteristic biomarkers. The interpretation of the biological significance of the biomarkers was finally achieved through the Human Metabolome Database (HMDB, <http://www.hmdb.ca>), Metlin (<http://metlin.scripps.edu>), massbank (<http://www.massbank.jp/>), LipidMaps (<http://www.lipidmaps.org>), mzccloud (<https://www.mzccloud.org>) and KEGG (<https://www.genome.jp/kegg/>) databases.

### 3.4. Statistical analysis

The experimental data of each group were statistically processed with SPSS 26.0 statistical software, and the results were expressed as mean  $\pm$  SD. One-way ANOVA was used for comparison between groups, LSD method was used for multiple comparisons, Dunnett's T3 comparison method was used for uneven variance, and  $P < 0.05$  was considered a significant difference.

## 4. Results

### 4.1. ASH analysis results

Compared with the self-established unified database for retention time and primary and secondary fragment ions, it was found that the main components of ASH were eleutheroside B, eleutheroside E, chlorogenic acid, oleuropein, isofraxidin and puerarin (Supplementary material 1).

### 4.2. ASH improves the behavior of PD model mice

Compared with the control group, the a-syn transgenic mice significantly decreased pole climbing and voluntary activity ( $P <$

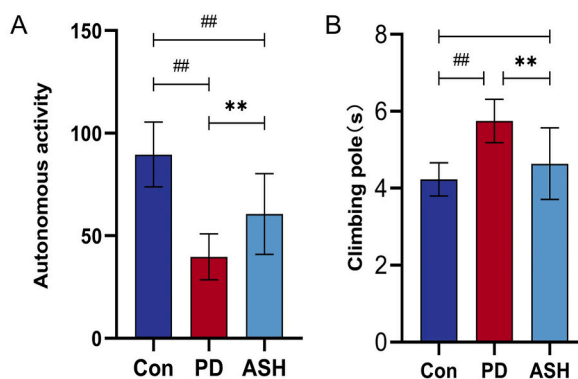


**Fig. 1.** Effects of ASH on rod climbing behavior (A) and autonomous activity (B) in mice (n = 9). Compared to the control group, ## $P < 0.01$ ; Compared to the model group, \*\* $P < 0.01$ .

0.01). After the intervention of ASH, the climbing speed became faster ( $P < 0.01$ ), and there was no difference compared with the control group (Fig. 1B). In addition, the autonomic activity times were increased ( $P < 0.01$ ), but not as much as that of the control group ( $P < 0.01$ ) (Fig. 1A). It suggested that ASH can alleviate the motor symptoms of Parkinson's patients.

4.3. Changes in gut microbiota after treatment with ASH

The Simpson index increased in the  $\alpha$ -syn transgenic mice group ( $P < 0.01$ ), and the administration of ASH can reduce the Simpson index ( $P < 0.01$ ), however the chao1, ACE, and Shannon indexes were not significantly different, indicating that the species diversity of the flora of the model group increased, and there was no significant difference in the abundance of the flora; however, ASH can return the intestinal microbial gut microbial species diversity (Fig. 2A). At the species level, PCA was performed on the ASH, Con, and PD groups. The ASH and Con groups were similar, and both groups had diversity in the structure of the flora from the PD group, indicating that the PD group's intestinal flora structure was different from that of the Con group, and ASH might improve this alteration (Fig. 2B).

Further analysis of microbial structural and compositional variation at the phylum and genus level was performed based on sequence data. Bacterial groups with >1% abundance in at least one sample were analyzed, and those with unsuccessful taxonomic

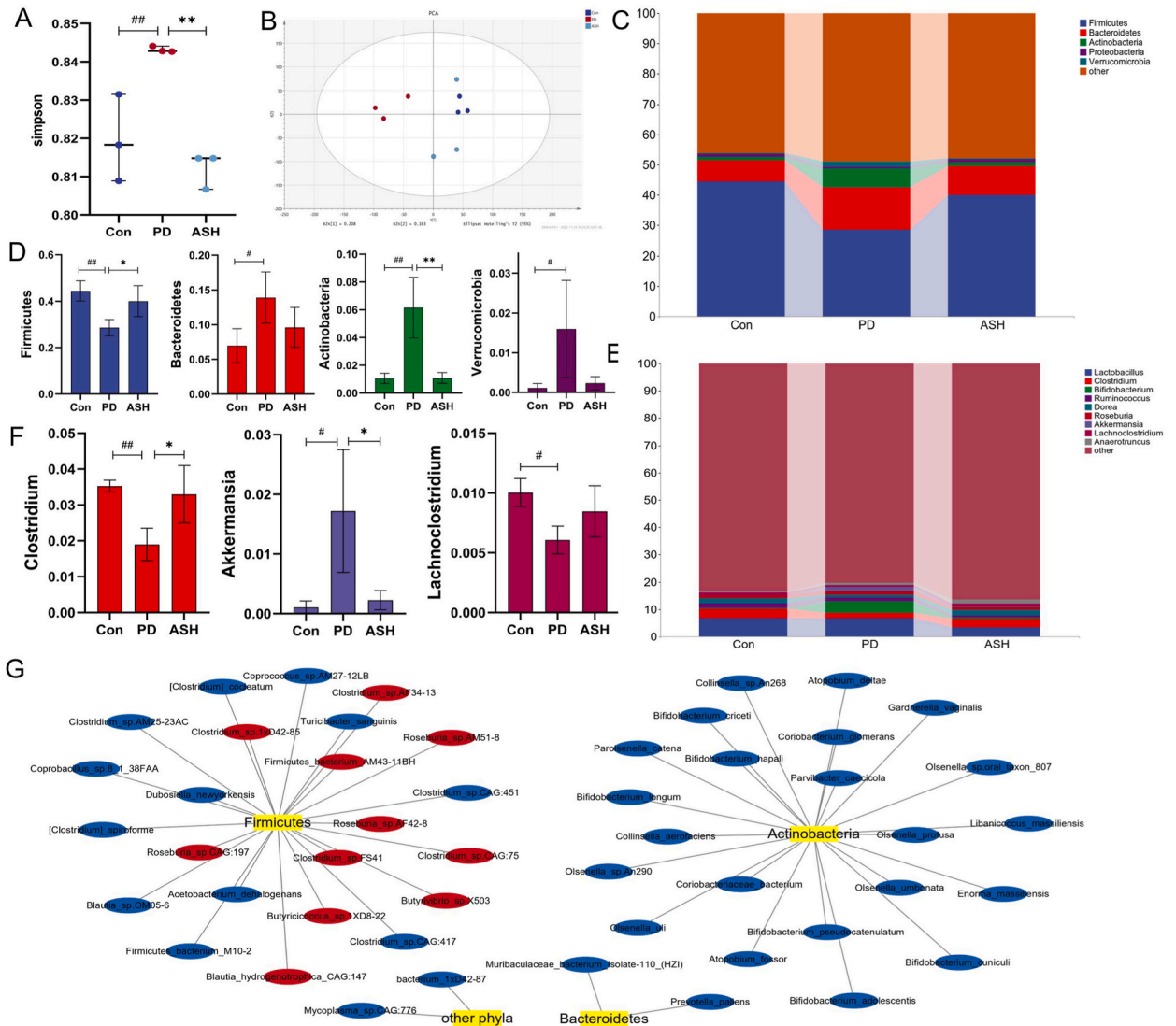
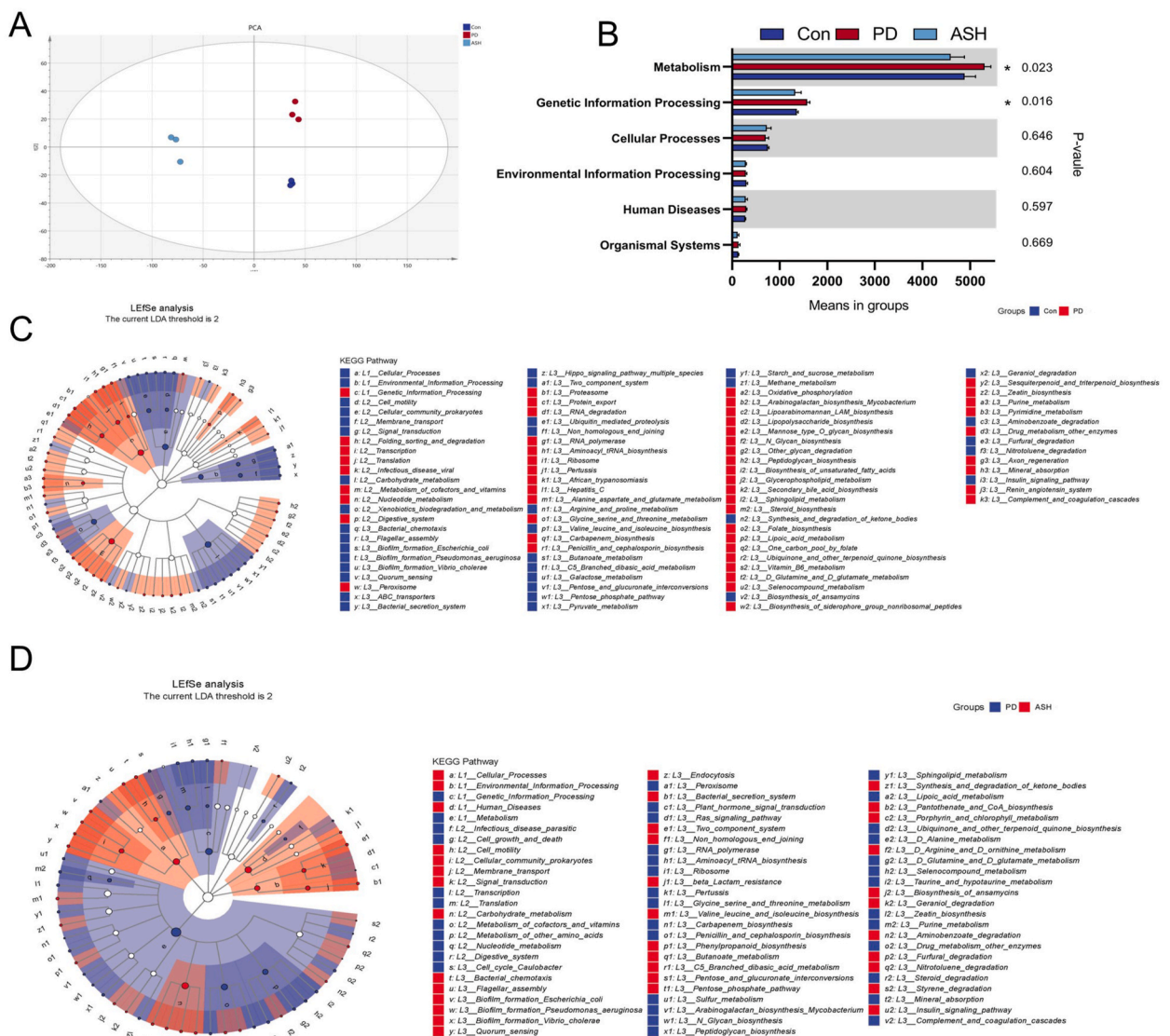


Fig. 2. Analysis of gut microbiota (n = 3). A: simpson index analysis; B: principal component analysis of species; C: species composition at the phylum level; D gut microbial variance analysis at phylum level, compared with the control group, ##P < 0.01, #P < 0.05, compared with the model group, \*\*P < 0.01, \*P < 0.05; E species composition at genus level; F: difference analysis of gut microbes at genus level, compared with control group, ##P < 0.01, #P < 0.05, compared with the model group, \*\*P < 0.01, \*P < 0.05; G species-level difference analysis of gut microbes, in which the red circle represents up-regulation compared with the model group, blue represents down-regulation, and yellow represents microbes Bacteria to which it belongs.

annotation were eliminated. *Firmicutes*, *Bacteroidetes*, *Actinobacteria*, *Proteobacteria*, and *Verrucomicrobia* were found to be the dominant groups at the phylum level (Fig. 2C). Compared with the control group, *Firmicutes* in  $\alpha$ -syn transgenic mice were significantly reduced ( $P < 0.01$ ), *Bacteroidetes*, *Verrucomicrobia*, and *Actinobacteria* significantly increased ( $P < 0.05$ , 0.01); *Firmicutes* were significantly increased ( $P < 0.05$ ) and *Actinobacteria* were significantly decreased ( $P < 0.01$ ) after intervention with ASH ( $P < 0.01$ ) (Fig. 2D). At the genus level, 9 dominant genera with an abundance greater than 1% were identified, namely *Lactobacillus*, *Clostridium*, *Bifidobacterium*, *Ruminococcus*, *Dorea*, *Roseburia*, *Akkermansia*, *LachnoClostridium*, *Anaerotruncus*. Among them, *Clostridium* and *LachnoClostridium* decreased significantly ( $P < 0.01$ , 0.05), and *Akkermansia* increased significantly ( $P < 0.05$ ) compared with the control group. The species abundances of *Clostridium* and *Akkermansia* decreased after the administration of ASH (Fig. 2E and F).

We analyzed the metagenomic data at the species level to search for specific microbial species that may mediate the treatment of PD with ASH. 18,204 species were annotated in the Con group, 18,462 in the ASH group, and 17,922 in the PD group. MetagenomeSeq was used to perform pairwise comparisons at the species level, and the differential species were screened for differences greater than 2-fold between groups ( $(\log_2(\text{Fold change value})) > 1$ ) and adjusted  $P < 0.05$ . The results revealed that 49 species underwent differential changes and back-regulation after the intervention of ASH, mainly from *Firmicutes*, *Actinobacteria*, and *Bacteroidetes* phyla



**Fig. 3.** Functional analysis of gut microbiota (n = 3). A: PCA analysis based on KOs level; B: Multi-group difference analysis based on KEGG1 level, \* $P < 0.05$ ; C: LefSe analysis of control group and PD group based on KEGG1-3 level; D: LefSe analysis of ASH group and PD group based on KEGG1-3 levels. E: Heatmap of the relative abundance of metabolism and gene information processing pathways (n = 3). LefSe analysis was performed on gut microbial functions at 3rd level of metabolic and genetic information processing in three groups, which were screened with LDA > 2 as the criterion to draw a heat map of relative abundance.

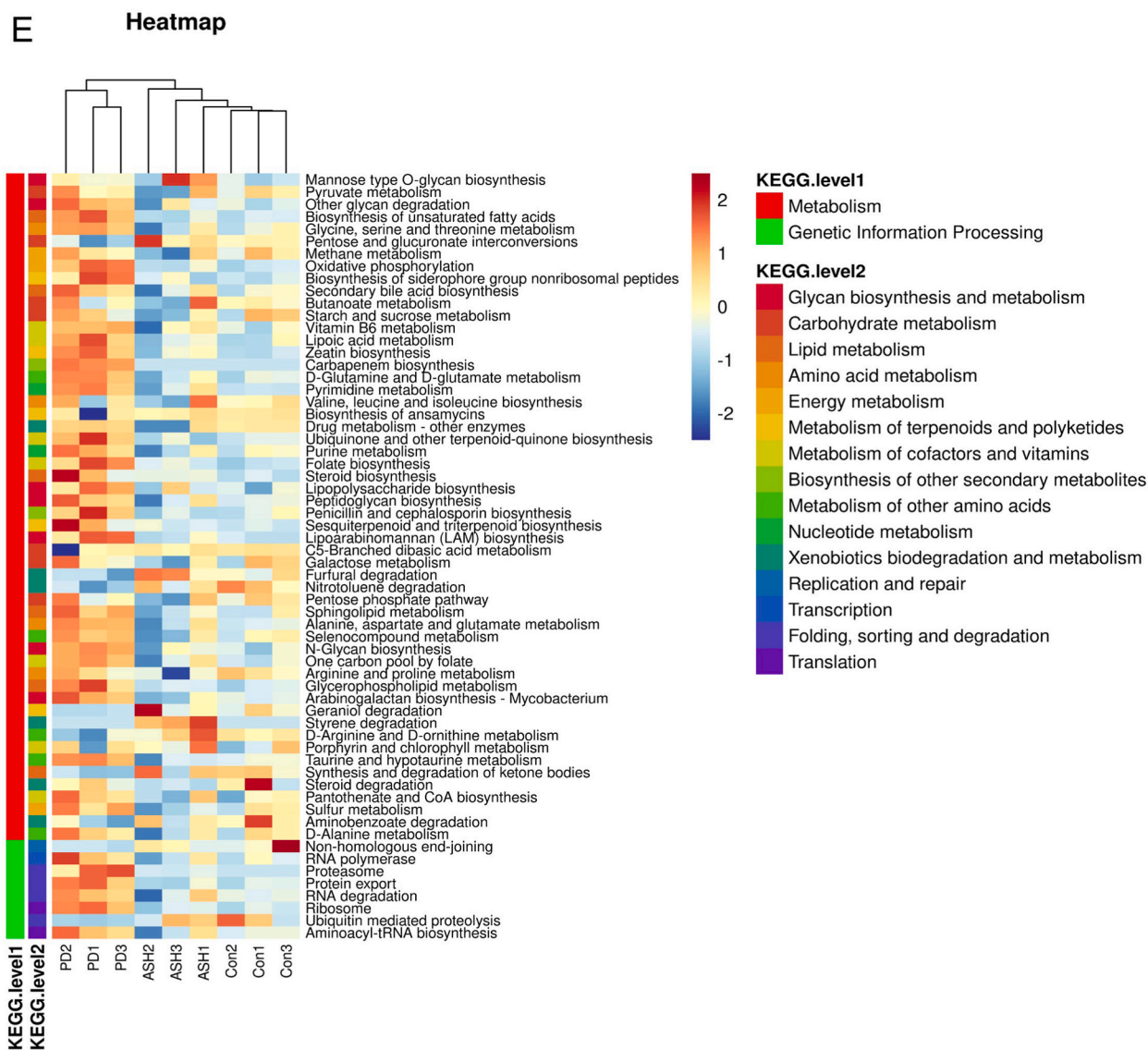


Fig. 3. (continued).

(Fig. 2G).

#### 4.4. ASH improves microbial function in PD model mice

Alterations in gut microbiota also caused potential functional changes; therefore, we further investigated the effects of ASH on the function of gut microbiota. Plotting PCA based on the KO results annotated by KEGG, the PD group and ASH group were separated (Fig. 3A). Comparative analysis at the level of KEGG1 revealed that metabolism and gene information processing pathways were the predominant pathways and the main pathway for the intervention of ASH (Fig. 3B). LEfSE analysis of KEGG with  $LDA > 2$  (Fig. 3C and D) screened a total of 52 metabolisms and gene information processing in the control and model groups at the KEGG3 level, of which 30 metabolism pathways were up-regulated and 14 were downregulated in the model group; 6 gene information processing pathways were upregulated and 2 were downregulated in the model group. The administration of ASH retraced 24 metabolism pathways and 4 gene information processing pathways (Fig. 3E).

#### 4.5. Metabolomics analysis

The above results indicated that the effect of ASH on the metabolism pathway was extremely significant, so we used UHPLC-Q-TOF-MS to detect further metabolites in the cecum contents of PD and ASH groups. To examine the repeatability and credibility of

sequencing, we used quality control samples (QC), and the Pearson analysis of the samples found that the correlation coefficient was greater than 0.99 under positive and negative ions, indicating that the data were stable and reliable throughout the detection process (Fig. 4A). In this study, 348 metabolites were identified in positive ion, and 248 metabolites were identified in negative ion mode, for a total of 541 metabolites identified in positive and negative ions. In the positive and negative ion modes, PCA results showed significant separation between each group (Fig. 4B), indicating significant differences in metabolites in PD mice after administering ASH. Prospective potential metabolites were screened with  $FC > 1.2$ ,  $P < 0.05$  or  $FC < 0.83$ ,  $P < 0.05$  (Fig. 4C). Subsequently, 13 biomarkers were screened with  $VIP > 1.0$  and  $P < 0.05$ , of which 8 were up-regulated, and 5 were down-regulated (Table 1).

On this basis, we enriched and analyzed the metabolic pathways of these 13 potential biomarkers through MetaboAnalyst5.0 (<https://www.metaboanalyst.ca>) to further evaluate the effects of ASH on metabolic pathways for PD treatment. Finally, 8 related metabolic pathways were obtained (Fig. 4D and E). The metabolic pathway's critical value was set at 0.05, and it was found that the ASH intervention targets were mostly involved in alpha-Linolenic acid metabolism. Additionally, unsaturated fatty acid biosynthesis, and purine metabolism are pathways for altered microbial function, with alpha-Linolenic acid (ALA) as a potential marker for alpha-Linolenic acid metabolism, and ALA, Palmitic acid, and Adenine as markers for unsaturated fatty acid biosynthesis and purine metabolism, respectively. The therapeutic impact of ASH may be achieved by changing the structure of intestinal flora and correcting the metabolic imbalance caused by PD.

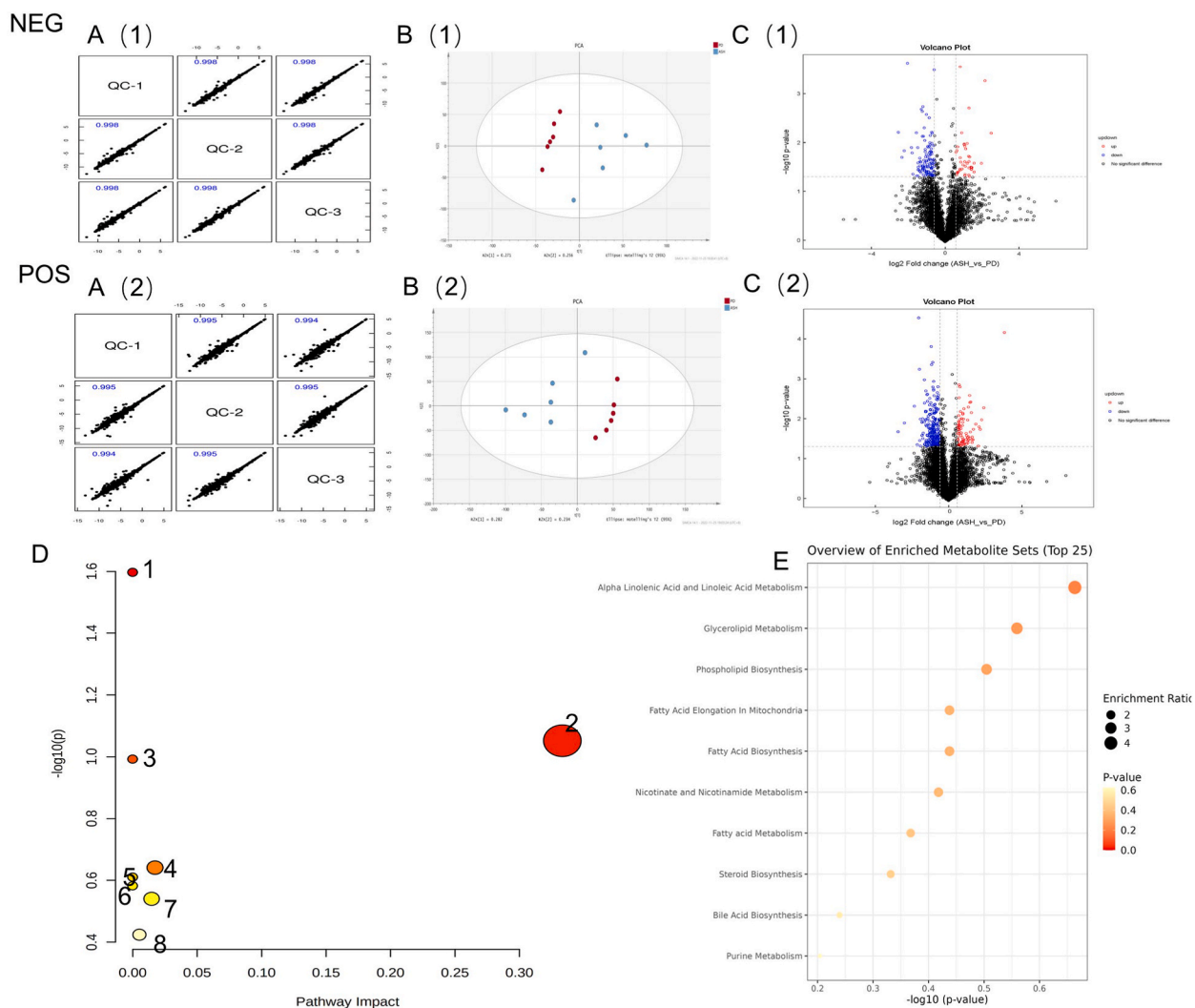


**Fig. 4.** Effects of ASH on fecal metabolites in PD mice (n = 6). (1) Negative ion mode, (2) Positive ion mode. A: Pearson analysis of QC samples; B: PCA analysis among three groups; C: Volcano plot between ASH group and PD group, Metabolites have significantly different with  $FC > 1.2$ ,  $P$  value  $< 0.05$  shown in rose, with  $FC < 0.83$  and  $P$  value  $< 0.05$  shown in blue. Non-significantly different metabolites are shown in black. D: Bubble diagram of differential metabolic pathways, 1. Biosynthesis of unsaturated fatty acids; 2. alpha-Linolenic acid metabolism; 3. Nicotinate and nicotinamide metabolism; 4. Glycerophospholipid metabolism; 5. Fatty acid; 6. Tyrosine metabolism; 7. Fatty acid biosynthesis; 8. Purine metabolism. E: Differential pathway enrichment analysis plot.

**Table 1**  
Potential biomarkers in PD mice.

| No. | ESI mode | Metabolites  | VIP      | Fold change | p-value | m/z      | rt(s)    | KEGG ID | HMDB        | ASH/PD |
|-----|----------|--|----------|-------------|---------|----------|----------|---------|-------------|--------|
| 1   | neg      | Quinate  | 1.487436 | 5.6288326   | 0.0009  | 191.056  | 343.161  | C00296  | HMDB0003072 | up     |
| 2   | neg      | DL-3-Phenyllactic acid                                     | 5.571457 | 2.0534264   | 0.0042  | 165.0559 | 119.232  | C01479  | HMDB0000779 | up     |
| 3   | neg      | Genisic acid   | 1.623248 | 0.6092293   | 0.0106  | 153.019  | 74.4915  | C00628  | HMDB0000152 | down   |
| 4   | neg      | Adenine  | 4.809586 | 1.8399568   | 0.0139  | 134.0468 | 165.6785 | C00147  | HMDB0000034 | up     |
| 5   | neg      | Palmitic acid  | 4.739869 | 0.8045787   | 0.0234  | 255.2337 | 45.595   | C00249  | HMDB0000220 | down   |
| 6   | neg      | Nicotinate   | 1.050987 | 1.2321228   | 0.0437  | 122.0245 | 224.624  | C00253  | HMDB0001488 | up     |
| 7   | pos      | Pro-Val  | 1.797349 | 4.776484    | 0.0011  | 215.1376 | 296.5    | –       | HMDB0029030 | up     |
| 8   | pos      | Ethyl 3-hydroxybutyrate                                    | 1.933163 | 5.0854447   | 0.0035  | 133.0847 | 63.269   | –       | HMDB0040409 | up     |
| 9   | pos      | Norharmaline   | 1.781143 | 1.4730464   | 0.0128  | 169.0745 | 146.927  | C20157  | HMDB0012897 | up     |
| 10  | pos      | Zingerone  | 1.0174   | 0.6349304   | 0.0177  | 389.191  | 215.5865 | C17497  | HMDB0032590 | down   |
| 11  | pos      | 1-Palmitoyl-sn-glycero-3-phosphocholine                    | 8.255866 | 1.2621803   | 0.0428  | 496.3388 | 190.967  | C04230  | HMDB0010382 | up     |
| 12  | pos      | 2,5,7,8-Tetramethyl-2-(beta-carboxyethyl)-6-hydroxychroman | 1.813641 | 0.5278932   | 0.0250  | 243.1325 | 350.748  | –       | HMDB0001518 | down   |
| 13  | pos      | alpha-Linolenic acid                                       | 2.544846 | 0.7563435   | 0.0450  | 279.2303 | 151.854  | C06427  | HMDB0001388 | down   |

#### 4.6. Correlation between gut microbes and differential metabolites after treatment with ASH

Since the major differential metabolites ALA, Adenine, and Palmitic acid are involved in 3 important metabolic pathways in the macrogenic functional analysis and metabolic pathway enrichment analysis, alpha-Linolenic acid metabolism, Biosynthesis of unsaturated fatty acids, and Purine metabolism. Therefore, we further investigated the correlation of 49 differential gut microbiotas with these 3 differential metabolites by Spearman correlation analysis with  $r > 0.7$  or  $r < -0.7$  and  $P < 0.05$  as screening conditions, it was found that Adenine was positively correlated with *Roseburia* sp. AF42-8 of *Firmicutes* phylum negatively correlated with *Collinsella aerofaciens* and *Coriobacterium glomerans* of *Actinobacteria* phylum. Palmitic acid was positively correlated with 7 species and negatively associated with 3 species; ALA was positively correlated with 7 species (Fig. 5A and B). These results suggest that ASH can improve the disturbance of gut microbiota during the development of PD and regulate unsaturated fatty acid production and purine metabolism pathway, suggesting that intestinal flora may play an important role in the treatment of PD by ASH.

## 5. Discussion

Parkinson's disease is a chronic and progressive degenerative disease of the central nervous system manifested by movement disorders. When misfolded  $\alpha$ -synuclein is deposited in the midbrain substantia nigra, degenerative changes occur in dopaminergic neurons, significantly reducing dopamine content, resulting in motor disorders such as resting tremor, myotonia, gait abnormality, and slow movement. Reduced levels of tyrosine carboxylase in the substantia nigra and striatum, as well as the numbers of dopaminergic neurons, can cause movement disorders (latency time for rotarod decreased, pole climbing time prolonged, the distance of movement and mean speed decreased), which are major neuropathological features of PD [16,17]. Eleutheroside B can increase the body's muscle glycogen reserve, so liver glycogen can decompose into glucose to maintain blood sugar concentration and ensure the energy required for exercise [18]. It can also remove free radicals from the body, reduce the leakage of LDH cells, improve SOD activity and reduce MDA content, to protect the body from oxidative stress and play a neuroprotective role [18,19]. Eleutheroside B and Eleutheroside E can inhibit the production and release of inflammatory cytokines such as TNF- $\alpha$ , IL-1 $\beta$ , IL-6 and NF- $\kappa$ B [20–23], to resist neuroinflammation in brain tissue and protect the integrity and stability of central nervous system [24], improving movement disorders. Improving motor coordination ability is an important standard to judge the effectiveness of PD drugs. The pole climbing experiment can reflect the motor coordination ability of animals [25,26]. If the motor coordination ability is strong, the pole can be grasped steadily, the movement is rapid, and the climbing time is short. However, PD animals need significantly more time due to muscle rigidity. In this experiment, the pole climbing time of PD group mice was significantly increased compared with the control group, suggesting that the motor coordination ability of PD group mice was impaired. After the intervention of ASH, the pole climbing time was significantly reduced, and there was no significant difference with the control group, indicating that ASH can improve the motor coordination ability of mice and has a protective effect on PD animal models. It is speculated that ASH can improve the symptoms of abnormal gait and slow movement by improving the motor balance ability of PD models.  $\alpha$ -synuclein aggregates are widely distributed in the sympathetic nerve (mediolateral column of cells and sympathetic ganglion) and the parasympathetic nerve center, causing autonomic nervous dysfunction and reduced limb activity in PD mice [27]. The number of free movements is a comprehensive index of dyspraxia (reduced motor function) caused by dopamine depletion [28]. The autonomic activity test can accurately record the number of horizontal and vertical movements of mice within a specified time, reflecting their voluntary movement ability. This experiment found that administering ASH could increase the number of autonomous activities of PD model mice during the test time. Although it could not recover to the control group level, ASH could antagonize the decrease of autonomous activities caused by  $\alpha$ -syn overexpression, increase the ability of voluntary movement, and improve the movement disorder of the PD model.

In this work, ASH can significantly improve the behavior of PD model mice. In order to elucidate the implication of ASH in treating

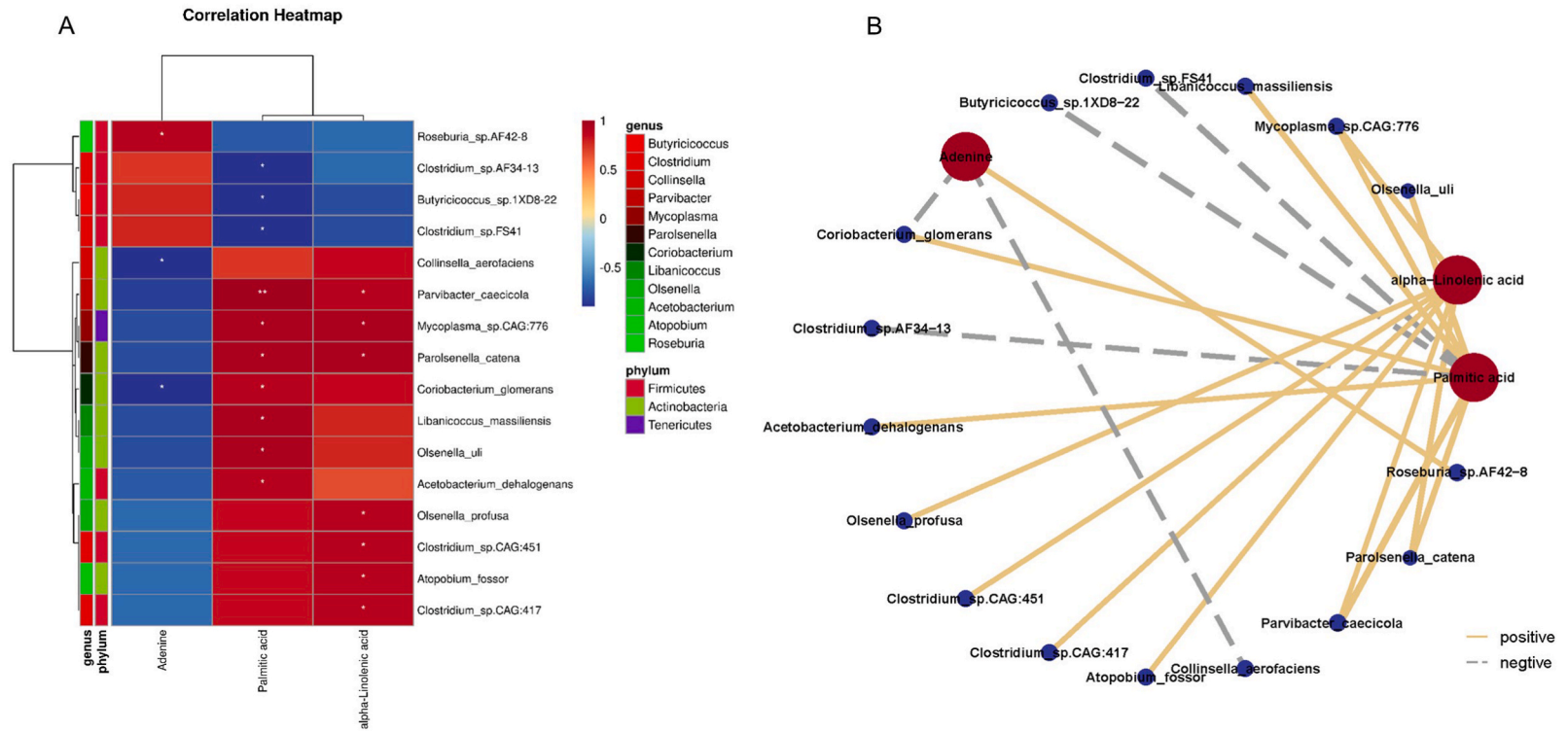


**Fig. 5.** Analysis of the correlation between metabolites and gut microbiotas. A: Spearman correlation analysis. Red squares indicate positive correlations, blue squares indicate negative correlations, the phylum and genus information for the selected species is shown on the left. B: Network diagram of the correlation between differential metabolites and strains. The thickness of the line represents the magnitude of the correlation, the yellow lines represent the positive correlation, the gray dotted line represents the negative correlation, the red dots represent the metabolites, and the blue-purple dots represent the progenitor species.

PD, we integrated metagenomic and fecal metabolomics to investigate the possible mechanism jointly. The results showed that ASH could improve metabolic disorders by regulating the structure and function of gut microbiotas in PD model mice, acting on alpha-Linolenic acid metabolism, unsaturated fatty acid production, and purine metabolism pathways. These results may provide new insights into treating PD with ASH, and targeting the gut microbiota and metabolic pathways may be a potential therapy for treating and preventing PD.

Eleutheroside E can regulate the changes of intestinal lactobacillus and *Helicobacter pylori* and reshape the intestinal microflora, while eleutheroside B may lose glucose and hydrolyze into syringaresinol under the action of intestinal microflora, which may be related to the dominant intestinal bacteria with hydrolyzed active enzymes, such as bifidobacterium and Lactobacillus. ASH may could modulate the structural composition of the gut microbiota to influence the PD process. Macro gene sequencing revealed that the gut microbiota diversity of PD model mice increased and *Firmicutes* significantly decreased; simultaneously, *Bacteroidetes*, *Verrucomicrobia*, and *Actinobacteria* significantly increased. *Firmicutes* and *Actinobacteria* were significantly back-regulated after ASH. *Firmicutes* is the largest group of intestinal microorganisms that ferment dietary fiber to produce short-chain fatty acids such as butyric acid, propionic acid, and acetic acid, which affect metabolism in multiple ways by acting on G protein-coupled receptors expressed by enteroendocrine cells [29], thereby reducing inflammatory factors such as TNF- $\alpha$  and reversing the PD process [30,31]. *Actinobacteria* is one of the most important and diverse phyla in the bacterial field, causing damage to dopaminergic neurons by producing protease inhibitors that prevent protein degradation [32]. The early and late onset of PD may be linked to the hibernation of *Actinobacteria* spores [33]. In this study, *Clostridium* and *lachnoClostridium* under the phylum *Firmicutes* in the model group decreased significantly, and *Akkermansia* increased significantly, which is also consistent with the research of Jing Sun [34], Sara Gerhardt [35], Zhe Zhao [36] and ASH can reverse *Clostridium*, *Akkermansia* changes. *Clostridium* can act on the GLP-1/GLP-1R pathway to improve dyskinesia in PD mice [34]. As PD progresses, the abundance of *Akkermansia* increases, and increased intestinal permeability increases the exposure of the enteric plexus to oxidative stress [37]. It also induces mitochondrial Ca<sup>2+</sup> overload in enteroendocrine cells, which causes phosphorylation and aggregation of a-syn proteins and promotes the development of PD [38]. Furthermore, matagenomeseq analysis revealed that ASH could recall 49 distinct strains, the majority of which are *Firmicutes*, *Actinobacteria*, and *Bacteroidetes*. However, what function do these various microbiotas have in PD? And how does ASH impact their therapeutic effects?

Therefore, we further analyzed the function of differential flora with the KEGG database, and the results showed that differential flora acted mainly on metabolism and gene information processing pathways. Also, ASH reversed 24 metabolism pathways and 4 gene information processing pathways altered in PD model mice. Consistent with previous findings, reduced the biosynthetic pathways of valine, leucine and isoleucine in PD patients, and the severity of PD was proportional to the reduction [39]. Valine, leucine, and isoleucine belong to branched-chain amino acids (BCAAs), which can quickly cross the blood-brain barrier and provide material N elements for the brain [40]. It can also participate in the "glutamate-BCAA cycle" between astrocytes and neurons through transamination, buffering potentially toxic levels of glutamate and maintaining the stability of the cerebral cistern [41]. In contrast, ASH enhances valine, leucine, and isoleucine biosynthetic pathways, preventing glutamate increases from over-activating glutamate receptors and increasing intracellular concentrations of Na<sup>+</sup> and Ca<sup>2+</sup> [42] to protect neurons and the CNS from toxic damage. Recent studies have highlighted the impact of DNA double-strand breaks on PD, with reactive oxygen species (ROS), a-synuclein, and damage to the DNA repair system [43,44], all of which may lead to DNA double-strand breaks, are important factors in accelerating neuronal damage [45]. Non-homologous DNA end joining (NHEJ), which repairs DNA double strands without an intact DNA template, is the primary pathway for DSBS repair in the brain [45,46]. In this study, ASH reversed the down-regulation of NHEJ caused by PD, which may promote the body to repair DNA double-strand breaks to protect neurons from damage. Therefore, ASH could alter the structure and composition of the gut microbiota and positively impact the metabolism and gene information processing pathways in order to regulate the development of PD.

Meanwhile, we have confirmed the positive role of ASH in maintaining metabolic homeostasis in PD model mice through fecal metabolomics analysis. Based on UHPLC-MS/MS analysis of the intestinal contents of mice in PD and ASH groups, we identified 13 differential metabolites and a knot metabolic pathway, alpha-Linolenic acid metabolism, as biomarkers of the pharmacological activity of ASH. ALA, the key metabolite of alpha-Linolenic acid metabolism, is an essential amino acid the human body requires. It inhibits the nuclear translocation of NF- $\kappa$ B caused by palmitic acid and the secretion of pro-inflammatory factors TNF- $\alpha$  and IL-6. Furthermore, it can also increase the expression of the antioxidant gene HO-1, reduce malondialdehyde and nitric oxide levels, and inhibit the production of ROS. ROS production and antioxidant effects [47,48] can inhibit the degeneration of dopaminergic neurons and improve movement disorders in PD [49]. In this study, alpha-Linolenic acid metabolism was down-regulated in the model group, resulting in the up-regulation of ALA levels, which could be used to counteract inflammation and oxidative stress in PD. ALA was not further up-regulated after the administration of ASH but showed a downward trend. It may be that ASH normalized the related inflammatory factors and oxidative stress indicators through other pathways, improving the inflammatory and oxidative stress response in PD, and the body's demand for ALA was reduced, hence the decreasing trend.

In addition, the differential metabolites ALA, Adenine, and Palmitic acid were mainly involved in purine metabolic pathways and unsaturated fatty acid synthesis, which got the same results as metagenomic functional analysis. In the present study, ASH improved purine metabolism and increased Adenine levels, which may result in increased urate production [50]. There is a negative correlation between uric acid and non-motor symptoms in PD patients [51]. The uric acid levels may reduce the uptake of dopamine transport ligands in the striatum and trigger idiopathic PD. As uric acid levels increase, PD patients are less likely to have dopaminergic deficits [52], and resistance to the neurotoxicity of 6-hydroxydopamine develops [53]. Palmitic acid, the most common saturated fatty acid in plant and animal species, has important biological functions such as storing energy, and maintaining cell membrane integrity. Increasing the oxidative stress of neurons and astrocytes [54] promotes TLR4 and the expression of pro-inflammatory cytokines, IL-6 and TNF- $\alpha$ , to activate NF- $\kappa$ B to induce neuroinflammation [55]. The administration of ASH promoted the unsaturated fatty acid

synthesis pathway, and the levels of palmitic acid and ALA in the feces decreased. Meanwhile, it was further demonstrated that alpha-Linolenic acid metabolism is a key pathway in the development of PD. Moreover, ALA and Palmitic acid are closely related to inflammation and oxidative stress of PD. In the absence of external interventions, the body counteracts the development of PD by self-help behaviors of increasing ALA intake, and the intervention of ASH can significantly reduce the inflammation and oxidative stress caused by Palmitic acid metabolism disorder, without the need for ALA intake to prevent and control the process of PD.

Overall, based on metagenomics and metabolomics, this experiment more comprehensively investigated the effect and mechanism of ASH in the treatment of PD, suggesting that ASH could improve the structure and function of the gut microbiota in PD mice and influence the fecal metabolic phenotypes. To further clarify the significance of ASH in the treatment of PD, we performed Spearman correlation analysis of the major differential gut microbiota from metagenome enrichment and metabolites ALA, adenine and palmitic acid obtained from metabolic pathway enrichment analysis. The findings revealed that ALA, adenine and palmitic acid were closely correlated with 16 species of Firmicutes, Tenericutes and Actinobacteria phylum, indicating that improving the composition of gut microbiota and maintaining undetermined metabolism may be the potential mechanisms of ASH for the treatment and prevention of PD. And these gut microbiota strains and ALA, adenine and palmitic acid could be ASH's key targets for treatment PD. It is important to note that eleutheroside B and eleutheroside E in ASH are inseparable from their effects, which could be one of the key factors for the realization of this regulatory effect.

## 6. Conclusion

In conclusion, this study explored the possible mechanism of ASH to improve the structure and function of gut microbiota in the PD model and regulate the metabolic disorder of PD. ASH mainly acts on the intestinal flora and fecal metabolism by regulating the flora abundance and species of Firmicutes, Tenericutes and Actinobacteria and improving markers of fecal metabolism, such as ALA, Adenine and Palmitic acid levels to affect alpha-Linolenic acid metabolism, unsaturated fatty acid synthesis, and purine metabolic pathways. These effects could regulate the motor behavior of PD model mice to a certain extent and may have an anti-PD impact, providing new targets and ideas for treating PD with ASH.

## Author contribution statement

Yi Lu: Conceived and designed the experiments; Analyzed and interpreted the data; Wrote the paper. Xin Gao: Conceived and designed the experiments; Performed the experiments; Wrote the paper. Yang Nan, Jiaqi Fu, Tianyu Wang: Performed the experiments. Chongzhi Wang, Chunsu Yuan: Analyzed and interpreted the data. Fang Lu: Analyzed and interpreted the data; Contributed reagents, materials, analysis tools or data. Shumin Liu: Contributed reagents, materials, analysis tools or data. Shadi A.D. Mohammed: Analyzed and interpreted the data; Wrote the paper.

## Data availability statement

Data associated with this study has been deposited at NCBI under the accession number PRJNA874173. The original contributions presented in the research are included in the article/supplementary material, and further queries can be directed to the corresponding authors.

## Ethics statement

The animal study was reviewed and approved by the institutional Animal Ethics Committee, Heilongjiang University of Chinese Medicine.

## Funding

This work was supported by the National Natural Science Foundation of China (No. 81774188, 82274125), the Heilongjiang Provincial Undergraduate Universities Central Supported Local Universities Reform and Development Fund, Harbin, China (No. 2021ZYQGLG001), and the Heilongjiang University of Traditional Chinese Medicine Outstanding Innovative Talents Support Program, Harbin, China.

## Declaration of competing interest

The authors declare that they have no known competing financial interests or personal relationships that could have appeared to influence the work reported in this paper.

## Appendix A. Supplementary data

Supplementary data related to this article can be found at <https://doi.org/10.1016/j.heliyon.2023.e18045>.

Supplementary material 1: A: ASH BPI chromatogram. B: Eleutheroside E identified in ASH. C: Standard of compound eleutheroside E. D: Oleuropein identified in ASH. E: Standard of compound oleuropein. F: Puerarin identified in ASH. G: Standard of compound

puerarin. H: Chlorogenic acid identified in ASH. I: Standard of compound chlorogenic acid. J: Isofraxidin identified in ASH. K: Standard of compound isofraxidin. L: Eleutheroside B identified in ASH. M: Standard of compound Eleutheroside B.

## References

- [1] R. Balestrino, A.H.V. Schapira, Parkinson disease, *Eur. J. Neurol.* 27 (1) (2020) 27–42.
- [2] C. Váradi, Clinical features of Parkinson's disease: the evolution of critical symptoms, *Biology* 9 (5) (2020) 103.
- [3] A. Samii, J.G. Nutt, B.R. Ransom, Parkinson's disease, *Lancet* 363 (9423) (2004) 1783–1793.
- [4] T.R. Sampson, et al., Gut microbiota regulate motor deficits and neuroinflammation in a model of Parkinson's disease, *Cell* 167 (6) (2016) 1469–1480.e12.
- [5] E.M. Klann, et al., The gut-brain Axis and its relation to Parkinson's disease: a review, *Front. Aging Neurosci.* 13 (2021), 782082.
- [6] F. Scheperjans, et al., Gut microbiota are related to Parkinson's disease and clinical phenotype, *Mov. Disord.* 30 (3) (2015) 350–358.
- [7] J.D. Mancini, et al., Gut microbiome changes with osteopathic treatment of constipation in Parkinson's disease: a pilot study, *Neurology (ECRicon)* 13 (2) (2021) 19–33.
- [8] W.A. Banks, et al., Lipopolysaccharide-induced blood-brain barrier disruption: roles of cyclooxygenase, oxidative stress, neuroinflammation, and elements of the neurovascular unit, *J. Neuroinflammation* 12 (2015) 223.
- [9] T. Ji, et al., Leveraging sequence-based faecal microbial community survey data to identify alterations in gut microbiota among patients with Parkinson's disease, *Eur. J. Neurosci.* 53 (2) (2021) 687–696.
- [10] R. Cai, et al., Enhancing glycolysis attenuates Parkinson's disease progression in models and clinical databases, *J. Clin. Invest.* 129 (10) (2019) 4539–4549.
- [11] S.N. Zhang, et al., Cerebral potential biomarkers discovery and metabolic pathways analysis of  $\alpha$ -synucleinopathies and the dual effects of *Acanthopanax senticosus* Harms on central nervous system through metabolomics analysis, *J. Ethnopharmacol.* 163 (2015) 264–272.
- [12] X.Z. Li, et al., Neuroprotective effects of extract of *Acanthopanax senticosus* Harms on SH-SY5Y cells overexpressing wild-type or A53T mutant  $\alpha$ -synuclein, *Phytomedicine* 21 (5) (2014) 704–711.
- [13] S.M. Liu, et al., *Acanthopanax senticosus* protects structure and function of mesencephalic mitochondria in A mouse model of Parkinson's disease, *Chin. J. Integr. Med.* 24 (11) (2018) 835–843.
- [14] S.M. Liu, et al., Protective effect of extract of *Acanthopanax senticosus* Harms on dopaminergic neurons in Parkinson's disease mice, *Phytomedicine* 19 (7) (2012) 631–638.
- [15] Y.D. Ren, et al., The effect of Baixanting compound on neuroinflammation in Parkinson's disease model mice, *China J. Trad. Chinese Med. Inform.* 22 (12) (2015) 68–71.
- [16] Y. Zuo, et al., Ferritinophagy-Mediated ferroptosis involved in paraquat-induced neurotoxicity of dopaminergic neurons: implication for neurotoxicity in PD, *Oxid. Med. Cell. Longev.* 2021 (2021), 9961628.
- [17] Y. Han, et al., Ginsenoside Rg3 exerts a neuroprotective effect in rotenone-induced Parkinson's disease mice via its anti-oxidative properties, *Eur. J. Pharmacol.* 909 (2021), 174413.
- [18] L. Wu, Q. Ye, L. Qi, Experimental study on anti-exercise fatigue effect of Eleutheroside B, *Northwest Pharmaceut. J.* 28 (1) (2013) 50–53.
- [19] Y. Dong, Neuroprotective effect of eleutheroside B on MPP+ injured PC12 cells, Beijing, in: 2014 Academic Annual Conference of Hospital Pharmacy Branch of Chinese Association of Traditional Chinese Medicine and International Academic Conference of TCM Professional Committee of World Association of Chinese Medicine, 2014.
- [20] F. Jie, et al., Stigmasterol attenuates inflammatory response of microglia via NF- $\kappa$ B and NLRP3 signaling by AMPK activation, *Biomed. Pharmacother.* 153 (2022), 113317.
- [21] J. Yao, et al., Synergistic cardioprotection by tiliainin and syringin in diabetic cardiomyopathy involves interaction of TLR4/NF- $\kappa$ B/NLRP3 and PGC1 $\alpha$ /SIRT3 pathways, *Int. Immunopharm.* 96 (2021), 107728.
- [22] C. He, et al., Eleutheroside E ameliorates arthritis severity in collagen-induced arthritis mice model by suppressing inflammatory cytokine release, *Inflammation* 37 (5) (2014) 1533–1543.
- [23] Y.C. Liu, et al., Anti-inflammatory and analgesic effects of eleutheroside E in alcoholic beverage, *J. Biol. Regul. Homeost. Agents* 33 (6) (2019) 1815–1821.
- [24] K. Belarbi, et al., Glycosphingolipids and neuroinflammation in Parkinson's disease, *Mol. Neurodegener.* 15 (1) (2020) 59.
- [25] H. Zhou, et al., Noninvasive ultrasound deep brain stimulation for the treatment of Parkinson's disease model mouse, *Research* 2019 (2019), 1748489.
- [26] S. Ferrazzo, et al., Increased anxiety-like behavior following circuit-specific catecholamine denervation in mice, *Neurobiol. Dis.* 125 (2019) 55–66.
- [27] J.L. Sabino-Carvalho, J.P. Fisher, L.C. Vianna, Autonomic function in patients with Parkinson's disease: from rest to exercise, *Front. Physiol.* 12 (2021), 626640.
- [28] T. Asakawa, et al., Animal behavioral assessments in current research of Parkinson's disease, *Neurosci. Biobehav. Rev.* 65 (2016) 63–94.
- [29] Y. Fan, O. Pedersen, Gut microbiota in human metabolic health and disease, *Nat. Rev. Microbiol.* 19 (1) (2021) 55–71.
- [30] T.B. Karunaratne, et al., Niacin and butyrate: nutraceuticals targeting dysbiosis and intestinal permeability in Parkinson's disease, *Nutrients* 13 (1) (2020) 28.
- [31] W. Feng, et al., Sodium butyrate attenuates diarrhea in weaned piglets and promotes tight junction protein expression in colon in a gpr109a-dependent manner, *Cell. Physiol. Biochem.* 47 (4) (2018) 1617–1629.
- [32] K.A. Caldwell, et al., Investigating bacterial sources of toxicity as an environmental contributor to dopaminergic neurodegeneration, *PLoS One* 4 (10) (2009) e7227.
- [33] K. Berstad, J.E.R. Berstad, Parkinson's disease; the hibernating spore hypothesis, *Med. Hypotheses* 104 (2017) 48–53.
- [34] J. Sun, et al., Probiotic *Clostridium butyricum* ameliorated motor deficits in a mouse model of Parkinson's disease via gut microbiota-GLP-1 pathway, *Brain Behav. Immun.* 91 (2021) 703–715.
- [35] S. Gerhardt, M.H. Mohajeri, Changes of colonic bacterial composition in Parkinson's disease and other neurodegenerative diseases, *Nutrients* 10 (6) (2018) 708.
- [36] Z. Zhao, et al., Fecal microbiota transplantation protects rotenone-induced Parkinson's disease mice via suppressing inflammation mediated by the lipopolysaccharide-TLR4 signaling pathway through the microbiota-gut-brain axis, *Microbiome* 9 (1) (2021) 226.
- [37] H. Nishiwaki, et al., Meta-analysis of gut dysbiosis in Parkinson's disease, *Mov. Disord.* 35 (9) (2020) 1626–1635.
- [38] D.P. Amorim Neto, et al., Akkermansia muciniphila induces mitochondrial calcium overload and  $\alpha$ -synuclein aggregation in an enteroendocrine cell line, *iScience* 25 (3) (2022), 103908.
- [39] Y. Zhang, et al., Plasma branched-chain and aromatic amino acids correlate with the gut microbiota and severity of Parkinson's disease, *NPJ Parkinsons Dis* 8 (1) (2022) 48.
- [40] C. Nie, et al., Branched chain amino acids: beyond nutrition metabolism, *Int. J. Mol. Sci.* 19 (4) (2018) 954.
- [41] M. Yudkoff, Interactions in the metabolism of glutamate and the branched-chain amino acids and ketoacids in the CNS, *Neurochem. Res.* 42 (1) (2017) 10–18.
- [42] J. Wang, et al., Molecular mechanisms of glutamate toxicity in Parkinson's disease, *Front. Neurosci.* 14 (2020), 585584.
- [43] M.T. Islam, Oxidative stress and mitochondrial dysfunction-linked neurodegenerative disorders, *Neurol. Res.* 39 (1) (2017) 73–82.
- [44] C. Milanese, et al., Activation of the DNA damage response in vivo in synucleinopathy models of Parkinson's disease, *Cell Death Dis.* 9 (8) (2018) 818.
- [45] D.K. Jeppesen, V.A. Bohr, T. Stevnsner, DNA repair deficiency in neurodegeneration, *Prog. Neurobiol.* 94 (2) (2011) 166–200.
- [46] H.H.Y. Chang, et al., Non-homologous DNA end joining and alternative pathways to double-strand break repair, *Nat. Rev. Mol. Cell Biol.* 18 (8) (2017) 495–506.
- [47] Y. Nan, M.N. Zhao, W. Zhang, Alpha-linolenic acid inhibits high-fat-induced oxidative stress and pro-inflammatory factor release in adipocytes, *J. Immunol.* 34 (11) (2018) 921–927.

- [48] N. Tofighi, et al., Protective effect of alpha-linoleic acid on A $\beta$ -induced oxidative stress, neuroinflammation, and memory impairment by alteration of  $\alpha 7$  nAChR and NMDAR gene expression in the hippocampus of rats, *Neurotoxicology* 85 (2021) 245–253.
- [49] S. Shashikumar, et al., Alpha-linolenic acid suppresses dopaminergic neurodegeneration induced by 6-OHDA in *C. elegans*, *Physiol. Behav.* 151 (2015) 563–569.
- [50] D. Zhang, et al., Production inhibition and excretion promotion of urate by fucoidan from *Laminaria japonica* in adenine-induced hyperuricemic mice, *Mar. Drugs* 16 (12) (2018) 472.
- [51] M. Moccia, et al., Is serum uric acid related to non-motor symptoms in de-novo Parkinson's disease patients? *Park. Relat. Disord.* 20 (7) (2014) 772–775.
- [52] M.A. Schwarzschild, et al., Serum urate and probability of dopaminergic deficit in early Parkinson's disease, *Mov. Disord.* 26 (10) (2011) 1864–1868.
- [53] M.R. Sarukhani, H. Haghdoost-Yazdi, G. Khandan-Chelarc, Changes in the serum urate level can predict the development of parkinsonism in the 6-hydroxy-dopamine animal model, *Neurochem. Res.* 43 (5) (2018) 1086–1095.
- [54] Y.W. Ng, Y.H. Say, Palmitic acid induces neurotoxicity and gliatotoxicity in SH-SY5Y human neuroblastoma and T98G human glioblastoma cells, *PeerJ* 6 (2018) e4696.
- [55] H. Amine, Y. Benomar, M. Taouis, Palmitic acid promotes resistin-induced insulin resistance and inflammation in SH-SY5Y human neuroblastoma, *Sci. Rep.* 11 (1) (2021) 5427.
- [56] C. Song, et al., *Acanthopanax senticosus* extract alleviates radiation-induced learning and memory impairment based on neurotransmitter-gut microbiota communication, *CNS Neurosci. Ther.* 29 (Suppl 1) (2023) 129–145.
- [57] Organization, W.H.. WHO monographs on selected medicinal plants Vol. 2., WHO, Geneva, 2002, pp. 83–96.
- [58] C. Song, et al., Eleutheroside E supplementation prevents radiation-induced cognitive impairment and activates PKA signaling via gut microbiota, *Commun. Biol.* 5 (1) (2022) 680.14.
- [59] C. He, et al., Eleutheroside E ameliorates arthritis severity in collagen-induced arthritis mice model by suppressing inflammatory cytokine release, *Inflammation* 37 (5) (2014) 1533–1543.
- [60] D. Yang, et al., The effect of Eleutheroside B on ERK1/2 of MPP $^{++}$ -induced PC12 cells, *J. Mol. Diagn. Ther.* 3 (2011) 155–158.
- [61] Y. He, et al., Chemical characterization of small-molecule inhibitors of monoamine oxidase B synthesized from the *Acanthopanax senticosus* root with affinity ultrafiltration mass spectrometry, *Rapid Commun. Mass Spectrom.* 34 (8) (2020) e8694.
- [62] K.M. Lau, et al., A review on the immunomodulatory activity of *Acanthopanax senticosus* and its active components, *Chin. Med.* 14 (2019) 25.
- [63] R. Dai, et al., Syringin alleviates ovalbumin-induced lung inflammation in BALB/c mice asthma model via NF- $\kappa$ B signaling pathway, *Environ. Toxicol.* 36 (3) (2021) 433–444.
- [64] D. Zhao, et al., Syringin exerts anti-inflammatory and antioxidant effects by regulating SIRT1 signaling in rat and cell models of acute myocardial infarction, *Immun. Inflamm. Dis.* 11 (2) (2023) e775.
- [65] Z. Shen, et al., Protective effects of syringin against oxidative stress and inflammation in diabetic pregnant rats via TLR4/MyD88/NF- $\kappa$ B signaling pathway, *Biomed. Pharmacother* 131 (2020) 110681.
- [66] Commission N.P.. Pharmacopoeia of the People's Republic of China, China Press of Traditional Chinese Medicine, Beijing, 2020, p. 215.